Preprints of the 19th World Congress
The International Federation of Automatic Control
Cape Town, South Africa. August 24-29, 2014

Fractional-order power rate type reaching law for sliding mode control of uncertain nonlinear system

Chun Yin * **YangQuan Chen** ** **Shou-ming Zhong** *

* *School of Mathematics Science, University of Electronic Science and Technology of China, Chengdu 611731, P. R. China (e-mail:* yinchun.86416@163.com*).*
** *Mechatronics, Embedded Systems and Automation (MESA) Lab, School of Engineering, University of California, Merced, 5200 North Lake Road, Merced, CA 95343, USA (e-mail:* yqchen@ieee.org; ychen53@ucmerced.edu*)*

Abstract: This paper develops a fractional-order (FO) power rate type reaching law for sliding mode control (SMC) of nonlinear integer order systems with disturbance and uncertainty. The proposed FO power rate type reaching law, including an FO derivative function, is proven to ensure that the state trajectories achieve to the switching surface in a finite time. Most importantly, the calculation formula of the reaching time under the FO reaching law is provided, for the first time. The comparisons between the FO and IO reaching laws reveal the potential advantages of the FO reaching law. Furthermore, the criterion for stability of the sliding mode dynamics is provided by solving linear matrix inequality (LMI). Finally, simulation and experimental examples illustrate the effectiveness and advantage of the proposed control method.

1. INTRODUCTION

Growing attention has been focused on fractional calculus [1, 2, 3] over the past three decades. FO calculus operators have recently become an exciting research topic in control area. The FO operators can help to design FO controllers which have a greater flexility in improving the control performance, such as robustness. This potential advantages have motivated renewed interest in various of FO control, such as [4, 5, 6].

On the other hand, SMC is famous to be computationally robust and efficient with respect to matched uncertainty and external disturbance [7, 8, 9]. The SMC includes two parts: equivalent control law and reaching law. However, due to the absence of appropriate mathematical methods, most published results about the FO SMC are limited to the FO equivalent control law, such as [10, 11, 12, 13]. It should be studied how to obtain useful tool for designing FO reaching law for the SMC. More importantly, it should be analyzed why and how to obtain a better control performance for SMC by using the FO reaching law.

With this motivation, an FO power rate reaching law is designed for SMC of uncertain nonlinear systems in this paper. A concept of the FO sign function $D^q\text{sgn}(s), 0 \leq q < 1$, including an FO differentiator, is applied to building an FO power rate type reaching law. Similar to the sign function, $D^q\text{sgn}(s), 0 \leq q < 1$, the fractional order derivative of $\text{sgn}(s)$, is proven to be able to extract the sign of s. One may feel this is trivial compared with the sign function itself; others may doubt that this is against intuition compared with the derivative of a generic function. It can guarantee the occurrence of the reaching phase in finite time. Furthermore, the calculation formula of the reaching time t_{reach} under the FO power rate type reaching law is obtained, for the first time. The comparison between the FO and IO power rate type reaching laws reveals the potential advantages of FO reaching law. Specially, the comparison is analyzed and visualized.

Next, the stability condition of the sliding mode dynamics is discussed. The matrices of the controlled system are derived by computing LMIs that are obtained from stability condition. As a result, a novel stability criteria is derived via LMIs. Finally, simulation and experimental examples are given to demonstrate the effectiveness and advantage of the designed control scheme.

2. PROBLEM FORMULATION AND PRELIMINARIES

Consider the nonlinear system with disturbance and uncertainty

$$\begin{aligned} \dot{x}(t) &= (A + \delta(t))x(t) + Ff(x,t) + Bu + Cw(t), \\ y(t) &= Dx(t), \end{aligned} \tag{1}$$

in which $x(t) \in R^n, u(t) \in R^\mu, y(t) \in R^\upsilon$ denote the state vector, the control input and the output. $w(t) \in R^m$ presents the norm-bounded external disturbance, satisfying $\|w(t)\| \leq b$ in which $b > 0$. $f(x,t) \in R^l$ is the nonlinear function. $A \in R^{n\times n}, F \in R^{n\times l}, B \in R^{n\times\mu}, C \in R^{n\times m}, D \in R^{\upsilon\times n}$ are constant known matrices. $\delta(t)$ is time-varying uncertain, which is assumed $\delta(t) = WG(t)N$, where W, N are constant known matrices, $G(t)$ satisfies $\|G(t)\| < 1, \forall t \geq 0$.

We need the following lemmas to derive the main results.

Lemma 1. [15] For constant matrices Π_1, Π_2, Π_3, in which $\Pi_1 = \Pi_1^T$, and $\Pi_2 = \Pi_2^T > 0$, then $\Pi_1 + \Pi_3^T\Pi_2^{-1}\Pi_3 < 0$ if and only if

$$\begin{bmatrix} \Pi_1 & \Pi_3^T \\ \Pi_3 & -\Pi_2 \end{bmatrix} < 0, \quad \text{or} \quad \begin{bmatrix} -\Pi_2 & \Pi_3 \\ \Pi_3^T & \Pi_1 \end{bmatrix} < 0. \tag{2}$$

Lemma 2. Consider $D^q s(t) = \frac{1}{\Gamma(1-\alpha)}\frac{d}{dt}\int_0^t \frac{s(\tau)}{(t-\tau)^q}d\tau, 0 \leq q < 1$ and sign function, one can conclude that

$$D^q\text{sgn}(s(t)) \begin{cases} > 0, \text{ if } s(t) > 0, t > 0, \\ < 0, \text{ if } s(t) < 0, t > 0. \end{cases}$$

Proof. See Appendix A.

A concept of $D^q\text{sgn}(s(t))$, involving an FO differentiator, is introduced to extract the sign of s.

Lemma 3. [14] For any matrix M_1 and M_2 of compatible dimensions and any scalar $\zeta > 0$, one has $M_1^T M_2 + M_2^T M_1 \leq \zeta M_1^T M_1 + (1/\zeta) M_2^T M_2$.

3. FO POWER RATE TYPE REACHING LAW FOR SMC

First, the sliding surface is choosing

$$s = C_1 x + C_2 z, \tag{3}$$

where $\dot{z} = Kx - z$ with $s \in R^\mu, z \in R^\iota, C_1 \in R^{\mu\times n}, C_2 \in R^{\mu\times\iota}, K \in R^{\iota\times n}$. Furthermore, C_1 should guarantee $C_1 B$ is not nonsingular. We define $|s|^l : R^\mu \to R^{\mu\times\mu}, \text{sgn}(s) : R^\mu \to R^\mu, D^q\text{sgn}(s) : R^\mu \to R^\mu$ as follows:

$$\begin{aligned} &|s|^l = \text{diag}\{|s_1|^l, |s_2|^l, \cdots, |s_\mu|^l\}, \\ &\text{sgn}(s) = [\text{sgn}(s_1), \text{sgn}(s_2), \cdots, \text{sgn}(s_\mu)]^T, \\ &D^q\text{sgn}(s) = [D^q\text{sgn}(s_1), D^q\text{sgn}(s_2), \cdots, D^q\text{sgn}(s_\mu)]^T, \end{aligned} \tag{4}$$

where $1 > q \geq 0$ and $1 > l > 0$. Then, a new FO power rate type reaching law is given by:

$$u_{reach} = -H|s|^l (D^q\text{sgn}(s)), 0 \leq q < 1, 0 < l < 1, \tag{5}$$

where $H = \text{diag}(h_1, h_2, \cdots, h_\mu)$, with $h_i > 0 (i = 1, \cdots, \mu)$.

Remark 4. The power rate type reaching law can improve the convergence rate when the state is away from the sliding surface. However, it decreases the speed when the state is close to it. Thus, it should be a low chattering and fast reaching mode. Furthermore, we will show the better control performance for the FO reaching law than IO one does in the following sections.

From (3) and (5), the SMC can be given

$$u = -(C_1 B)^{-1}[(C_1 A + C_2 K + C_1)x + C_1 F f(x,t) + \bar{u}], \tag{6}$$

in which $\bar{u} = w_1 - s$, with $w_1 = (\|C_1 W\| \|Nx\| + b||C_1 C||)\text{sgn}(s) + H|s|^l D^q\text{sgn}(s)$.

4. REACHABILITY ANALYSIS

4.1 Finite time convergence analysis

Next, the reachability analysis of the sliding surface will be considered.

Theorem 5. Consider the system (1) and switching surface (3), the state trajectories via SMC (6) can reach $s(t) = 0$.

Proof. Consider the Lyapunov function $V(t) = s^T(t)s(t)$. Taking the differentiating with respect to time, we have

$$\dot{V} = [C_1\dot{x} + C_2\dot{z}]^T s + s^T[C_1\dot{x} + C_2\dot{z}]. \tag{7}$$

Substitution of (1) and (6) into (7) yields

$$\dot{V} = [C_1\delta(t)x + C_1 C w - w_1]^T s + s^T[C_1\delta(t)x + C_1 C w - w_1].$$

Since $\|G(t)\| < 1, ||w|| < d$, one has from $\|G(t)\| < 1, ||w|| < d$

$$\begin{aligned} \dot{V} &\leq \Omega + \Omega^T - (s^T H|s|^l D^q\text{sgn}(s) + (H|s|^l D^q\text{sgn}(s))^T s) \\ &\leq -(s^T H|s|^l D^q\text{sgn}(s) + (H|s|^l D^q\text{sgn}(s))^T s), \end{aligned} \tag{8}$$

where $\Omega = s^T C_1\delta(t)x + s^T C_1 C w - s^T \|C_1 W\| \|Nx\| \text{sgn}(s) - bs^T \|C_1 C\| \text{sgn}(s)$. From Lemma 2, one has $\dot{V} \leq 0$. Thus, the states of system (1) under the controller (6) can achieve to the predefined switching surface in finite time.

4.2 Calculation formula of reaching time

First, we consider the sliding surface $s(t) \in R$. Then, we have $0.5\dot{V} = s\dot{s} \leq -h|s|^l s D^q\text{sgn}(s) \leq 0$ in which $0 \leq q < 1, 0 < l < 1$ and h is positive constant.

Let $s\dot{s} = -h|s|^l s D^q\text{sgn}(s) \leq 0$. Before deriving t_{reach} under the FO reaching law, t_{reach} under the corresponding IO power rate type reaching law $u_{reach} = -h|s|^l\text{sgn}(s)$ will be calculated. For the IO power rate reaching law, one has $s\dot{s} = -h|s|^l s\text{sgn}(s) \leq 0$. There are two cases:

1). When the initial condition $s(0)$ is bigger than 0,

$$\dot{s}(t) = -hs^l \Rightarrow \dot{s}s^{-l} = -h, \tag{9}$$

So one has $\left(s^{1-l}\right)' = -(1-l)h$. Thus, the following equation can be obtained

$$s^{1-l}(t) = s^{1-l}(0) - (1-l)ht, \tag{10}$$

Since $s(t_{reach}) = 0$, one has $t_{reach} = s^{1-l}(0)/(1-l)h$.

2). When the initial condition $s(0)$ is smaller than 0,

$$-\dot{s}(-s)^{-l} = -h \Rightarrow \left(\frac{(-s)^{1-l}}{1-l}\right)' = -h, \tag{11}$$

So one has $\left((-s)^{1-l}\right)' = -(1-l)h$. The integration of this equation is given as

$$(-s(t))^{1-l} = (-s(0))^{1-l} - (1-l)ht, \tag{12}$$

Since $s(t_{reach}) = 0$, one has $t_{reach} = (-s(0))^{1-l}/(1-l)h$.

According to **1)** and **2)**, one has

$$t_{reach} = |s(0)|^{1-l}/(1-l)h. \tag{13}$$

Similarly, t_{reach} under the FO power rate type reaching law can be calculated. Consider two cases:

3). When $s(0) > 0$, one has $\dot{s}s^{-l} = -hD^q\text{sgn}(s)$. Thus, $s^{1-l}(t) - s^{1-l}(0) = -\frac{(1-l)ht^{1-q}}{(1-q)\Gamma(1-q)}$. Since $s(t_{reach}) = 0$, one has

$$t_{reach} = \left(\frac{(1-q)\Gamma(1-q)s^{1-l}(0)}{(1-l)h}\right)^{\frac{1}{1-q}}.$$

4). When $s(0) < 0$, one has $\dot{s}(-s)^{-l} = -hD^q\text{sgn}(s)$. Thus, one has

$$t_{reach} = \left(\frac{(1-q)\Gamma(1-q)(-s(0))^{1-l}}{(1-l)h}\right)^{1/1-q}.$$

Therefore, according to **3)** and **4)**, the reaching time under the FO power rate type reaching law is

$$t_{reach} = \left(\frac{(1-q)\Gamma(1-q)|s(0)|^{1-l}}{(1-l)h}\right)^{\frac{1}{1-q}}. \tag{14}$$

Table 1. **Calculation formulae** of reaching time under the power rate type reaching laws

Power rate type reaching law	Reaching time (t_{reach})
IO power rate version	$\frac{\lvert s(0)\rvert^{1-l}}{(1-l)h}$
FO power rate version	$\left(\frac{(1-q)\Gamma(1-q)\lvert s(0)\rvert^{1-l}}{(1-l)h}\right)^{\frac{1}{1-q}}$

Next, for $s = [s_1(t), s_2(t), \cdots, s_\mu(t)]^T \in R^\mu$, t^i_{reach} of $s_i(t), (i = 1, 2, \cdots, \mu)$ under the FO power rate reaching law can be obtained

$$t^i_{reach} = \left(\frac{(1-q)\Gamma(1-q)(-s_i(0))^{1-l}}{(1-l)h_i}\right)^{\frac{1}{1-q}}. \quad (15)$$

Hence, the reach time $t_{reach} = \max\{t^i_{reach}, i = 1, \cdots, \mu\}$.

4.3 The comparison of the FO/IO power rate type reaching laws

The **calculation formulae** of t_{reach} under the FO and IO power rate type reaching laws are listed in Table 1. The FO power rate type reaching law with $D^q\text{sgn}(s), 0 \le q < 1$ is the FO/IO reaching law synthesis (IO controller with $\text{sgn}(s)$ and FO controller with $D^q\text{sgn}(s), 0 < q < 1$).

One important aspect of the good reaching control performance is to obtain a shorter reaching time. In order to show how to obtain a faster convergence performance, the following remark is presented in detail.

Remark 6. The FO sign function is the reason why t_{reach} under the FO reaching law can be smaller than the IO one does. Specifically, from the proof of Lemma 2, there exists a series of q such that $|D^q\text{sgn}(s)| > 1$ during the initial time interval. (*For example, when* $s(t) > 0$, *for* $\forall t \in [0, 0.2]$, *the changes in* $D^q\text{sgn}(s)$ *along with* q, t *are depicted in Fig. 1. It shows that* $D^q\text{sgn}(s) > 1 = \text{sgn}(s), 0 < q \le 0.98$ *during the initial time interval.*) Thus, the reaching dynamics determined by the FO power rate type reaching law can create a stronger push toward the sliding surface. The simulation and experimental examples can illustrate the advantage of the proposed controller.

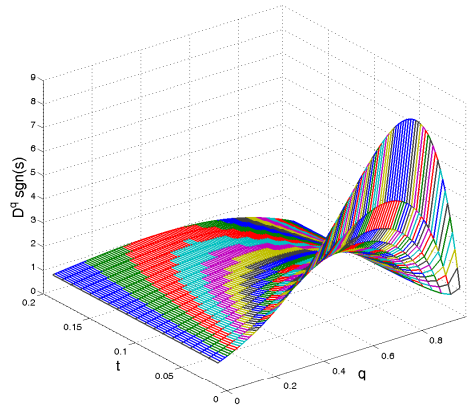

Fig. 1. Relationship between $D^q\text{sgn}(s)$ and q, for $s(t) > 0, 0 \le q \le 0.98$.

5. STABILITY ANALYSIS

In the section, the stability analysis of sliding mode dynamics will be investigated. For simplicity, define the matrix: $\tilde{N} = [N_1^T \ N_2^T \ N_3^T \ N_4^T]^T$.

Theorem 7. The sliding mode dynamics is asymptotically stable if there exist $\bar{P} > 0$, any matrices $N_i, (i = 1, 2, 3, 4)$ with appropriate dimensions and $\varepsilon_1, \varepsilon_2 > 0$, satisfying the following LMI:

$$\begin{bmatrix} \Psi_{11} & * & * & * & * & * & * & * & * \\ \Psi_{21} & \Psi_{22} & * & * & * & * & * & * & * \\ \Psi_{31} & \Psi_{32} & \Psi_{33} & * & * & * & * & * & * \\ \Psi_{41} & \Psi_{42} & \Psi_{43} & \Psi_{44} & * & * & * & * & * \\ N & 0 & 0 & 0 & \Psi_{55} & * & * & * & * \\ \Psi_{61} & 0 & 0 & 0 & 0 & \Psi_{66} & * & * & * \\ 0 & \Psi_{72} & 0 & 0 & 0 & 0 & \Psi_{77} & * & * \\ 0 & 0 & \Psi_{83} & 0 & 0 & 0 & 0 & \Psi_{88} & * \\ 0 & 0 & 0 & \Psi_{94} & 0 & 0 & 0 & 0 & \Psi_{99} \end{bmatrix} < 0, \quad (16)$$

where

$\Psi_{11} = N_1E + E^TN_1^T + \bar{P}E + E^T\bar{P} + \varepsilon_2N^TN$,
$\Psi_{21} = N_2E + W^TN_1^T, \Psi_{22} = N_2W + W^TN_2^T - \varepsilon_1I$,
$\Psi_{31} = N_3E + C^TN_1^T + C^T\bar{P}, \Psi_{32} = N_3W + C^TN_2^T$,
$\Psi_{33} = N_3C + C^TN_3^T, \Psi_{41} = N_4E - N_1^T$,
$\Psi_{42} = N_4W - N_2^T, \Psi_{43} = N_4C - N_3^T, \Psi_{44} = -N_4 - N_4^T$,
$\Psi_{55} = -(\varepsilon_1I)^{-1}, \Psi_{61} = W^T\bar{P}, \Psi_{66} = -\varepsilon_2I$,
$\Psi_{72} = W^T\bar{P}, \Psi_{77} = -\varepsilon_2I, \Psi_{83} = W^T\bar{P}, \Psi_{88} = -\varepsilon_2I$,
$\Psi_{94} = W^T\bar{P}, \Psi_{99} = -\varepsilon_2I, E = -C_1^{-1}C_2K - I$.

Proof. Since the overall closed-loop dynamics is dependent on the control law, the sliding mode dynamics can be derived

$$\dot{x} = (-C_1^{-1}C_2K - I + \delta(t))x(t) + Cw(t). \quad (17)$$

For simplicity, define $p(t) = G(t)q(t) = G(t)Nx(t)$. Then, the system (17) is rewritten by $\dot{x} = Ex(t) + Wp(t) + Cw(t)$, where $E = -C_1^{-1}C_2K - I$. Define the augmented vector $\eta(t) = [x^T(t) \ \ p^T(t) \ \ w^T(t) \ \ \dot{x}^T(t)]^T$. Construct the Lyapunov function $V(x(t)) = x^T\bar{P}x$, in which $\bar{P} > 0$. The time derivative of V is obtained

$$\dot{V} = \eta^T(t)\left\{\begin{bmatrix} E^T\bar{P} + \bar{P}E & * & * & * \\ 0 & 0 & * & * \\ (\bar{P}C)^T & 0 & 0 & * \\ 0 & 0 & 0 & 0 \end{bmatrix} + \begin{bmatrix} \delta(t)^T\bar{P} + \bar{P}\delta(t) & * & * & * \\ 0 & 0 & * & * \\ 0 & 0 & 0 & * \\ 0 & 0 & 0 & 0 \end{bmatrix}\right\}\eta(t). \quad (18)$$

Considering the uncertainty in the second matrix of the left side of the equation (18), from Lemma 3, one has

$$\begin{bmatrix} \bar{P}WG(t)N + (WG(t)N)^T\bar{P} & * & * & * \\ 0 & 0 & * & * \\ 0 & 0 & 0 & * \\ 0 & 0 & 0 & 0 \end{bmatrix}$$
$$\le \frac{1}{\varepsilon_2}\begin{bmatrix} \bar{P}W & * & * & * \\ 0 & \bar{P}W & * & * \\ 0 & 0 & \bar{P}W & * \\ 0 & 0 & 0 & \bar{P}W \end{bmatrix}\begin{bmatrix} W^T\bar{P} & * & * & * \\ 0 & W^T\bar{P} & * & * \\ 0 & 0 & W^T\bar{P} & * \\ 0 & 0 & 0 & W^T\bar{P} \end{bmatrix}$$
$$+\varepsilon_2\begin{bmatrix} N^TN & * & * & * \\ 0 & 0 & * & * \\ 0 & 0 & 0 & * \\ 0 & 0 & 0 & 0 \end{bmatrix}, \text{in which } \varepsilon_2 > 0. \quad (19)$$

The following inequality is obtained

$$p^T(t)p(t) \le \eta^T(t)\bar{N}^T\bar{N}\eta(t), \quad (20)$$

where $\bar{N}$=[N 0 0 0]. In order to get less conservative, the zero equation is used

$$2\eta^T\tilde{N}(Ex+Wp+Cw-\dot{x})=\eta^T\Pi\eta=0, \tag{21}$$

where

$$\Phi=\begin{bmatrix}\Phi_{11} & * & * & *\\ \Phi_{21} & \Phi_{22} & * & *\\ \Phi_{31} & \Phi_{32} & \Phi_{33} & *\\ \Phi_{41} & \Phi_{42} & \Phi_{43} & \Phi_{44}\end{bmatrix},$$
$$\Phi_{11}=N_1E+E^TN_1^T, \Phi_{21}=N_2E+W^TN_1^T,$$
$$\Phi_{22}=N_2W+W^TN_2^T, \Phi_{31}=N_3E+C^TN_1^T,$$
$$\Phi_{32}=N_3W+C^TN_2^T, \Phi_{33}=N_3C+C^TN_3^T,$$
$$\Phi_{41}=N_4E-N_1^T, \Phi_{42}=N_4W-N_2^T,$$
$$\Phi_{43}=N_4C-N_3^T, \Phi_{44}=-N_4-N_4^T.$$

Using the S-procedure, suppose there exists $\varepsilon_1>0$ satisfying

$$\begin{bmatrix}\delta(t)^T\bar{P}+\bar{P}\delta(t) & * & * & *\\ 0 & 0 & * & *\\ 0 & 0 & 0 & *\\ 0 & 0 & 0 & 0\end{bmatrix}+\varepsilon_2\begin{bmatrix}N^TN & * & * & *\\ 0 & 0 & * & *\\ 0 & 0 & 0 & *\\ 0 & 0 & 0 & 0\end{bmatrix}$$
$$-\begin{bmatrix}0 & * & * & *\\ 0 & \varepsilon_1 I & * & *\\ 0 & 0 & 0 & *\\ 0 & 0 & 0 & 0\end{bmatrix}+\tilde{N}^T\varepsilon_1 I\tilde{N}+\begin{bmatrix}\Phi_{11} & * & * & *\\ \Phi_{21} & \Phi_{22} & * & *\\ \Phi_{31} & \Phi_{32} & \Phi_{33} & *\\ \Phi_{41} & \Phi_{42} & \Phi_{43} & \Phi_{44}\end{bmatrix}$$
$$+\frac{1}{\varepsilon_2}\begin{bmatrix}\bar{P}W & * & * & *\\ 0 & \bar{P}W & * & *\\ 0 & 0 & \bar{P}W & *\\ 0 & 0 & 0 & \bar{P}W\end{bmatrix}\begin{bmatrix}W^T\bar{P} & * & * & *\\ 0 & W^T\bar{P} & * & *\\ 0 & 0 & W^T\bar{P} & *\\ 0 & 0 & 0 & W^T\bar{P}\end{bmatrix}$$
$$<0, \tag{22}$$

then, we have $\dot{V}\leq 0$. By Lemma 2, the inequality (22) can be hold if the inequality (8) exists. Hence, it guarantees the sliding mode dynamics asymptotic stability.

6. SIMULATION

Two examples are utilized to show the advantage and applicability of the proposed control methods.

Example 1. Consider the double-integrator plant

$$\begin{cases}\dot{x}_1=x_2,\\ \dot{x}_2=u,\end{cases} \tag{23}$$

The initial state is set as $x0=[0.5,0.5]^T$, the switching surface and the FO reaching law are proposed as

$$s=c_1x_1+c_2x_2, \tag{24}$$
$$\dot{s}=c_1\dot{x}_1+c_2\dot{x}_2=slaw, \tag{25}$$

in which $slaw=-h|s|^lD^q\text{sgn}(s)$ is the FO power rate reaching law, the parameters $c_1=5, c_2=1, h=10$ and $q=0.2$. The Hurwitz condition $c_1>0$ guarantees the sliding mode dynamics stable. Substituting (22) into (25), the following FO SMC can be obtained $u=-5x_2-10|s|^lD^q\text{sgn}(s)$. Using this controller, the phase trajectory of sliding mode, the time responses of s, x_1, x_2 are separately shown in parts (a), (b), (c), (d) of Fig. 2. The time response of u is depicted in Fig. 3.

So as to show the advantage of the FO power rate type reaching law, the simulations are performed while q is changed. $x^i=[x_1^i,x_2^i]^T, (i=0,1,2,3)$ denote the states of the system (22) via the SMC based on the FO power rate type reaching law with different q_i (i.e. $q_0=0, q_1=0.2, q_2=0.34, q_3=0.42$). The phase trajectories of x^i, s^i under the FO SMC are given in Fig.4. The time responses of x_1^i, x_2^i are plotted in Fig.5. It shows that the FO power rate type reaching law can have a better control performance.

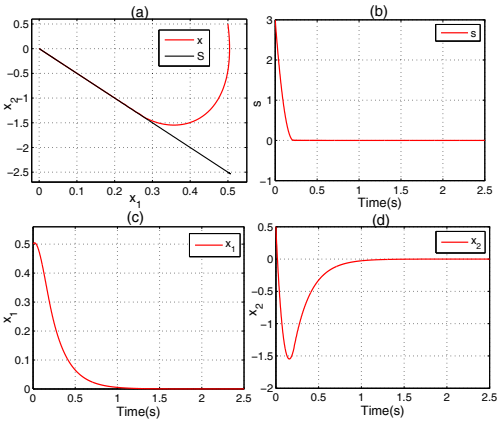

Fig. 2. (a) Phase trajectory of the state x under the FO power rate type reaching law and sliding surface S; (b) the time response s; (c) the time response x_1 and (d) the time response of x_2.

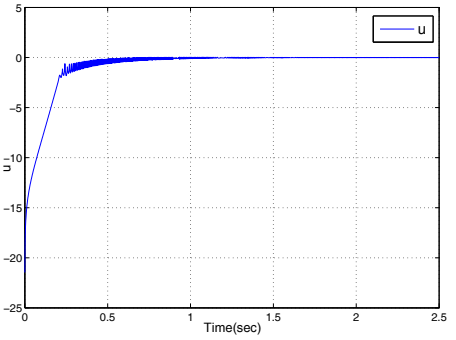

Fig. 3. The time response of SMC with FO power rate type reaching law.

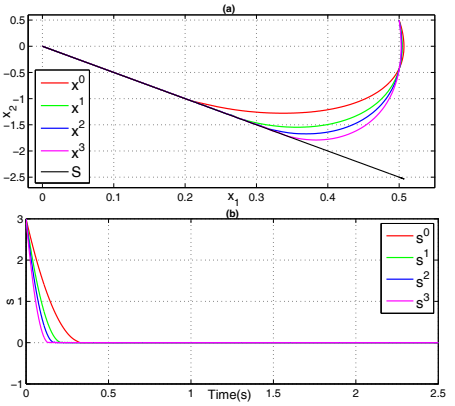

Fig. 4. (a)Phase trajectories of the states $x^i, (i=0,1,2,3)$ under SMC with $q_i=0, 0.2, 0.34, 0.42$ and S; (b)the time responses of $s^i, (i=0,1,2,3)$.

Example 2. Consider Chua's circuit ([15])

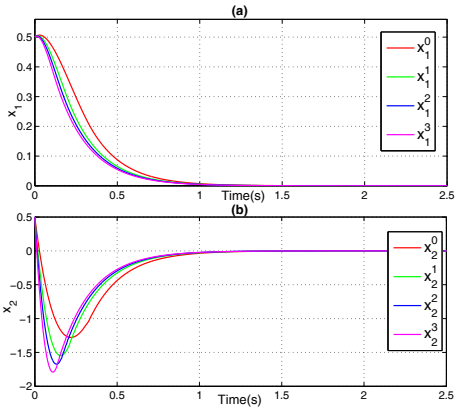

Fig. 5. The time responses of $x_1^i, x_2^i, (i = 0, 1, 2, 3)$.

$$\dot{x} = \left\{ \begin{bmatrix} 18/7 & 9 & 0 \\ 1 & -1 & 1 \\ 0 & -14.78 & 0 \end{bmatrix} + \delta(t) \right\} x + \begin{bmatrix} 1 & 0 & 0 \\ 0 & 1 & 0 \\ 0 & 0 & 1 \end{bmatrix} \begin{bmatrix} f(x_1) \\ 0 \\ 0 \end{bmatrix} + \begin{bmatrix} 1 & 0 & 1 \\ 0 & 1 & 1 \\ 0 & 0 & 1 \end{bmatrix} u(t), \tag{26}$$

in which $f(x_1) = 0.5(n_0 - n_1)(|x_1 + \varpi| - |x_1 - \varpi|)$ with $\varpi = 1, n_0 = -1/7, n_1 = 2/7, \beta = 0.2$. The uncertainty $\delta(t) = WG(t)N$ with

$$W = N = \begin{bmatrix} 1 & 0 & 0 \\ 0 & 1 & 0 \\ 0 & 0 & 1 \end{bmatrix}, G(t) = \begin{bmatrix} \tilde{\delta} & 0 & 0 \\ 0 & \tilde{\delta} & 0 \\ 0 & 0 & \tilde{\delta} \end{bmatrix}.$$

where $\tilde{\delta} = 0.1 \sin(0.1t)$. Let

$$C_1 = -\begin{bmatrix} 0.5639 & 0 & 0 \\ 0 & 0.5639 & 0 \\ 0 & 0 & 0.5639 \end{bmatrix}, C_2 = \begin{bmatrix} 1 & 0 & 0 \\ 0 & 1 & 0 \\ 0 & 0 & 1 \end{bmatrix},$$
$$H = \begin{bmatrix} 0.18 & 0 & 0 \\ 0 & 0.18 & 0 \\ 0 & 0 & 0.18 \end{bmatrix}.$$

By using Theorem 7, a feasible solution of the symmetric matrice and scalars is found using LMI Control Toolbox:

$$K = -\begin{bmatrix} 4.3510 & 0 & 0 \\ 0 & 3.6941 & 0 \\ 0 & 0 & 1.5869 \end{bmatrix}, \varepsilon_1 = 0.3278, \varepsilon_2 = 0.5819.$$

By using (11), we can obtain the following SMC law:

$$u = \begin{bmatrix} -5.6302 & -23.2800 & 3.8142 \\ -1.0000 & -20.8310 & 2.8412 \\ 0 & 14.7800 & -3.8412 \end{bmatrix} x - \begin{bmatrix} 1 & 0 & -1 \\ 0 & 1 & -1 \\ 0 & 0 & 1 \end{bmatrix} f(x,t) + \begin{bmatrix} \kappa & 0 & -\kappa \\ 0 & \kappa & -\kappa \\ 0 & 0 & \kappa \end{bmatrix} \bar{u}, \tag{27}$$

where $\kappa = 1.7734, \bar{u} = 0.5639||Nx||\text{sgn}(s) + HD^q\text{sgn}(s) - s$ with $q = 0.12$. By Theorem 5, the system (26) under the controller (27) converges to the sliding surface:

$$s = -\begin{bmatrix} 0.5639 & 0 & 0 \\ 0 & 0.5639 & 0 \\ 0 & 0 & 0.5639 \end{bmatrix} x + \begin{bmatrix} 1 & 0 & 0 \\ 0 & 1 & 0 \\ 0 & 0 & 1 \end{bmatrix} z,$$
$$\dot{z} = -\begin{bmatrix} 4.3510 & 0 & 0 \\ 0 & 3.6941 & 0 \\ 0 & 0 & 1.5869 \end{bmatrix} x - \begin{bmatrix} 1 & 0 & 0 \\ 0 & 1 & 0 \\ 0 & 0 & 1 \end{bmatrix} z. \tag{28}$$

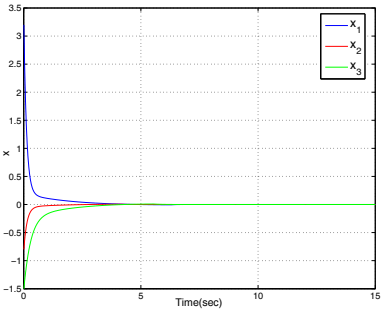

Fig. 6. Time responses of states for the system (26) via the FO SMC (27).

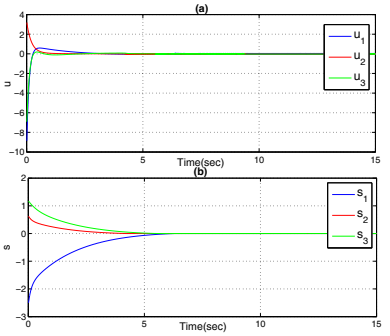

Fig. 7. (a) Time responses of the controller (27); (b) time responses of the sliding surface (28).

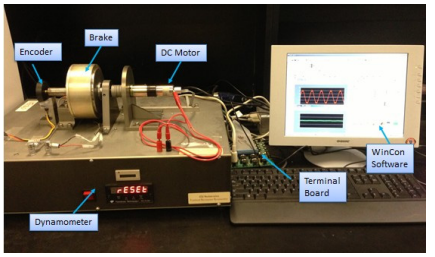

Fig. 8. The fractional horse power dynamometer.

The initial condition is $[3.2, -0.8, -1.5]^T$. Fig. 6 shows the time responses of x_1, x_2, x_3 under the controller (27). The time responses of the switching surface (28) and SMC(27) are drawn in Fig. 7. It is obvious that the designed controller asymptotically stabilizes the unstable Chua's system.

7. EXPERIMENT

Experimental example is presented of applying the FO SMC with the FO power rate type reaching law on a fractional horsepower dynamometer ([16]). In Fig. 8, the dynamometer has a DC motor, an optical encoder, a hysteresis brake, a tachometer. It communicates with a Quanser Multi-Q3 terminal board for the connect with the Matlab/Simulink Real-Time Workshop environment through WinCon 4.0. The DC motor in dynamometer is identified as

$$G_m(s) = \frac{1.52}{1.01s + 1}. \tag{29}$$

In order to show the effectiveness of the FO reaching law, we perform a position tracking control by SMC with the FO reaching law. Let the reference signal $r(t) =$

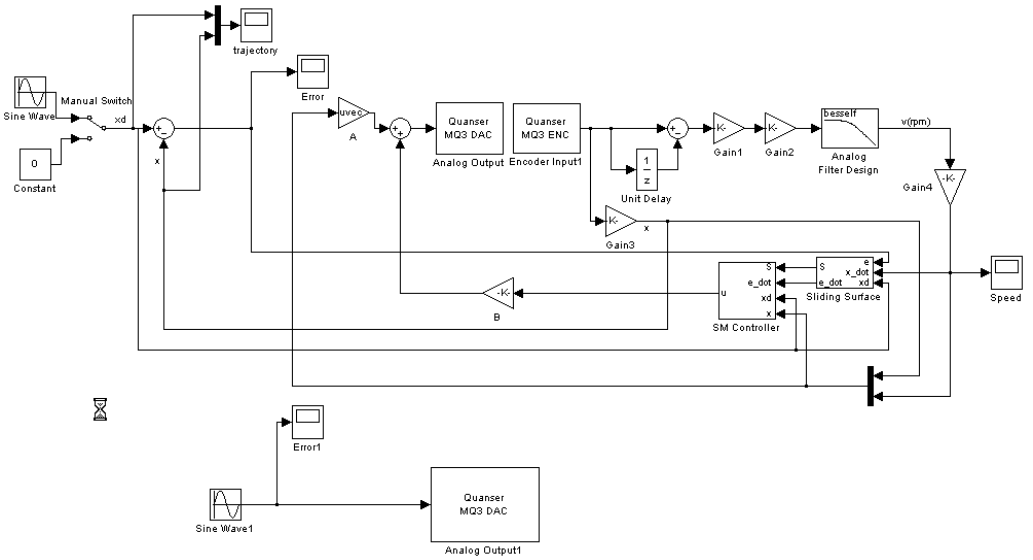

Fig. 9. Simulink/RTW model built in the SMC experiment.

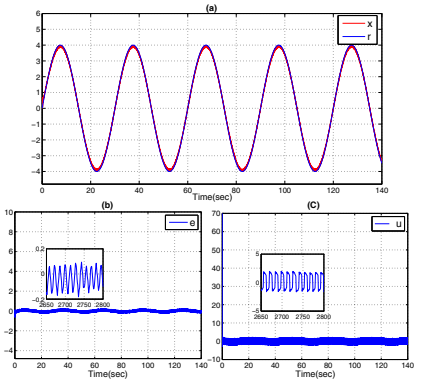

Fig. 10. Position tracking under the FO power rate reaching law with $q = 0.1$.

$4\sin(2\pi/40)$. The FO reaching law and sliding surface are defined as $u_{reach} = -0.85|s|^{0.1}D^q\text{sgn}(s)$ and $s = e + \dot{e}$ in which $e = r - x_1$. The Simulink/RTW model built for the experiment is shown in Fig. 9. The tracking is performed in Fig. 10. As illustrated in Fig. 9, the disturbance sin(t) is added to the Magtrol Hysteresis Brake in order to test the robust property of the FO reaching law. The experimental results show the applicability of the proposed control methods.

8. CONCLUSION

The FO SMC with the FO power rate type reaching law has been proposed for nonlinear systems with disturbance and uncertainty. The FO power rate type reaching law has proven to ensure the occurrence of the reaching phase in finite time. The calculation formula of the reaching time has been provided. The stability criterion for the sliding mode dynamics has been derived by solving LMIs. Simulation and experimental examples have been presented to illustrate the effectiveness and advantage of the designed control method.

REFERENCES

[1] I. Podlubny. *Fractional Differential Equations.* New York: Academic Press, 1999.

[2] A. A. Kilbas, H. M. Srivastava, and J. J. Trujillo. *Theory and Applications of Fractional Differential Equations.* Amsterdam, Netherlands: Elsevier, 2006.

[3] Y. Li, Y. Q. Chen and I. Podlubny. Mittag-Leffler stability of fractional order nonlinear dynamic systems. *Automatica*, 45, pages 1965–1969, 2009.

[4] I. Podlubny. Fractional-order systems and $PI^{\lambda}D^{\mu}$-controllers. *Nonlinear Analysis: Theory, Methods & Applications*, 69, pages 2677–2682, 1999.

[5] Y. Luo, and Y. Q. Chen. Stabilizing and robust fractional order PI controller synthesis for first order plus time delay systems. *Automatica*, 48, pages 2159–2167, 2012.

[6] C. Yin, B. Stark, Y.Q. Chen, and S. Zhong. Adaptive minimum energy cognitive lighting control: integer order vs fractional order strategies in sliding mode based extremum seeking. *Mechatronics*, 23, pages 863–872, 2013.

[7] V. I. Utkin. *Sliding Modes in Control and Optimization.* New York: Springer-Verlag, 1992.

[8] C. Edwards and S.K. Spurgeon. *Sliding Mode Control: Theory and Applications.* London: Taylor & Francis, 1998.

[9] H. H. Choi. LMI-based sliding surface design for integral sliding mode control of mismatched uncertain systems. *IEEE Trans Automat Control* 52, pages 736–42, 2007.

[10] M. S. Tavazoei, and M. Haeri. Synchronization of chaotic fractional-order systems via active sliding mode controller. *Physica A: Statistical Mechanics and its Applications*, 387, pages 57–70, 2008.

[11] S. H. Hosseinnia, R. Ghaderia, A. Ranjbar N., M. Mahmoudiana, S. Momani. Sliding mode synchronization of an uncertain fractional order chaotic system. *Computers & Mathematics with Applications*,59, pages 1637–1643, 2010.

[12] M. P. Aghababa, S. Khanmohammadi, and G. Alizadeh. Finite-time synchronization of two different chaotic systems with unknown parameters via sliding mode technique. *Applied Mathematical Modelling*, 35, pages 3080–3091, 2011.

[13] C. Yin, Y. Q. Chen, and S.M. Zhong. LMI based design of a sliding mode controller for a class of uncertain fractional-order nonlinear systems. in *Proceedings of the 2013 American Control Conference*, pages 6526-6531, 2013.

[14] S. Boyd, L. E. Ghaoui, E. Feron, and V. Balakrishnan. *Linear Matrix Inequalities in System and Control Theory.* SIAM, Philadelphia, PA, 1994.

[15] C. Yin, S. M. Zhong, and W. Chen. Robust H_∞ control for uncertain Lur'e systems with sector and slope restricted nonlinearities by PD state feedback. *Nonlinear Analysis Real World Applications*, 12, pages 501-512, 2011.

[16] Y. Tarte, Y. Q. Chen, W. Ren, and K. Moore. Fractional horsepower dynamometer-a general pupose hardware-in-the-loop real-time simulation platform for nonlinear ontrol research and education. in *Proc. 45th IEEE Conference on Decision and Control*, pages 7113–7118, 2006.

Appendix A. PROOF OF LEMMA 2

Omitted due to space limit.